Proceedings Paper:

Smith, M.J., Gladwin, D.T. orcid.org/0000-0001-7195-5435 and Stone, D.A. orcid.org/0000-0002-5770-3917 (2016) Experimental analysis of dynamic charge acceptance test conditions for lead-acid cells. In: IECON Proceedings (Industrial Electronics Conference). IECON 2016 - 42nd Annual Conference of the IEEE Industrial Electronics Society, 24/10/16 - 27/10/16, Florence. IEEE , pp. 2046-2051. ISBN 9781509034741

https://doi.org/10.1109/IECON.2016.7793307

Experimental Analysis of Dynamic Charge Acceptance Test Conditions for Lead-Acid Cells

M. J. Smith, D. T. Gladwin and D. A. Stone
Electrical Machines and Drives Research Group,
Department of Electronic and Electrical Engineering,
University of Sheffield, Sheffield, UK
Email: matt.j.smith@sheffield.ac.uk

***Abstract*—This paper presents the results of a series of tests to determine the Dynamic Charge Acceptance (DCA) performance of small form-factor 2 V, 6 Ah, carbon-enhanced VRLA cells designed for Hybrid Electric Vehicle (HEV) applications. A test procedure has been written for a battery test system, based on a modified DCA Short Test profile. Results have been obtained for a batch of cells, tested at various temperatures, rest periods and states of charge. These conditions have been chosen to mimic a range of real-life scenarios which could potentially be encountered during HEV operation. The resulting analysis demonstrates clear variations and trends in DCA performance which may be used to inform conditions for future testing regimes. The same test procedure is then applied to standard lead-acid cells and the results compared.**

I. Introduction

Recent years have seen battery technology and performance become increasingly important in automotive applications. Driven by a desire to reduce emissions and rises in fuel costs, the function of automotive batteries has shifted from an auxiliary power source to providing significant contributions to the performance of the vehicle; particularly in the case of fully electric vehicles (EV), where it is the only source of energy. This, coupled with increasingly power-hungry driver-aids, entertainment and HVAC systems is making it increasingly important that the behaviour of automotive batteries be well understood.

A. Battery Use in Vehicles

In traditional internal-combustion (IC) engined vehicles the battery is used exclusively as an auxiliary energy store for when the engine is switched off, once running the engine provides all power for the vehicle, both mechanical via the drive-train and electrical via the alternator. In this configuration the battery is subject to infrequent, short discharges at high currents (around 16 times the 1-hour rate, C_1) when starting the engine, followed by modest recharging to full state-of-charge (SoC) at around 1 C_1 from the alternator [1]. The use of automotive batteries for starting, lighting and ignition (SLI) and their failure modes under these conditions is well understood.

An increasingly common modification to this method of working is the stop-start system. Here the IC engine is stopped automatically when the vehicle is stationary, and re-started before moving off. This system is designed to reduce the time the engine spends running whilst the vehicle is stationary, thus reducing fuel usage and emissions. Whilst this imposes a more demanding duty on the batteries due to the increased frequency of the discharge-charge cycles experienced by the battery, the fundamental operating mode and recharging mechanism remains the same.

More significant changes to battery operation are imposed by hybrid electric vehicles (HEV). In such vehicles the IC engine is used in conjunction with the batteries such that both provide traction power. There are several configurations possible for the drive arrangement of such vehicles [2], but the principle of operation is similar; the vehicle may be driven by either the engine or batteries alone, or by the two together. This allows such vehicles to drive quietly and with zero emissions at low speeds, such as within cities. It also means they can be fitted with smaller, more efficient IC engines sufficient for most driving, but maintain performance when accelerating by using their batteries to increase available power.

As the batteries are by necessity much larger in a HEV than in a conventional vehicle, an alternator is not sufficient to recharge them. Therefore recharging is performed by using the electrical machine fitted within the drive-train as a generator [2]. This allows the batteries to be recharged by the IC engine through the drive system, but also allows energy to be stored in the batteries when the vehicle brakes.

This modifies significantly the loads imposed on the battery. Aside from the large discharges associated with starting the IC engine, there are additional discharge spikes caused by acceleration as well as longer periods of lower discharge currents where the vehicle is running in purely electric mode. The charging profile is similarly modified, the batteries are no longer steadily charged back to full SoC, instead operation is often at partial SoC. Charging from the engine is controlled to a modest rate, but is interspersed with large charge spikes due the regenerative braking system; these spikes can reach up to 30 C_1 under heavy braking [1]. The operation of batteries under these conditions of high-rate partial-state-of-charge (HRPSoC) is becoming increasingly common as the number of HEV's increases.

B. Charge Acceptance

It can be seen from the above that to maximise the effectiveness of the HEV drive-train, as much energy as possible

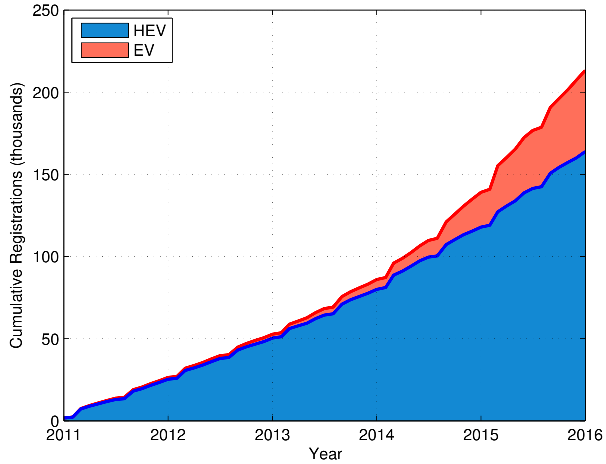

Fig. 1: UK EV Registrations, Jan. 2011 – Jan. 2016[1]

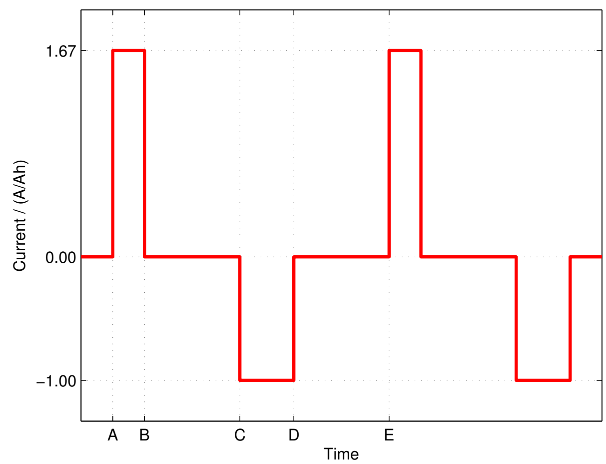

Fig. 2: DCA Test A3 Microcycle Current Profile (A – E)

must be recaptured and stored during any and all regenerative braking periods. The main factor limiting the ability to capture this energy is the charge acceptance of the batteries at HRPSoC. As the batteries used in automotive applications are being required to provide more of the electrical power to the vehicle it is crucial that they are able to be recharged sufficiently quickly and that the performance of batteries under these conditions is known.

Understanding the Dynamic Charge Acceptance (DCA) performance of automotive batteries has been identified as a key requirement for the development of electric vehicles [3]–[5], and standard test procedures have been designed to characterise the DCA performance of batteries [6]. Lithium-based cells dominate this sector, but concerns relating to cost, safety and a lack of recycling infrastructure persist. This paper presents the results of an investigation into how varying the conditions and parameters of the standard DCA test regime effects the results and aims to show that advanced lead-acid cells can be a viable solution for HEV applications.

II. DCA Overview

DCA is a measure of the charge efficiency of a battery, the higher the DCA value the better the charge efficiency. The standard test for determining DCA performance involves the application of a defined current waveform to the battery under test, the response of the battery to this waveform is used to calculate DCA performance.

A. Microcycling

At the heart of the DCA test is the microcycle, it is this which defines the current applied to the battery, and from which the performance may be determined. The standard microcycle, as defined by the DCA Test A3 specification [6] is given in Figure 2.

[1]Compiled from the Society of Motor Manufacturers and Traders '*EV and AFV Registrations*' (2011 & 12) and '*EV Registrations*' (2012, 13, 14, 15 & 16) data.

TABLE I: DCA Test A3 Microcycle Current Profile Procedure

Step	Description
1, (A – B)	Charge at 1.67 A·Ah^{-1} with voltage limit of 2.47 V per cell for 10 s
2, (B – C)	Rest 30 s
3, (C – D)	Discharge at 1.00 A·Ah^{-1} until charge added in Step 1 is removed
4, (D – E)	Rest 30 s

DCA performance is determined by the response of the battery to the charge phase of the microcycle (step 1). During this phase the test procedure attempts to charge the battery with a current of 1.67 A·Ah^{-1} for 10 seconds, this will cause the terminal voltage of the battery to rise. If during the charge step the voltage reaches the set limit of 2.47 V per cell (equivalent to 14.8 V for a standard 6 cell battery) the charge current is reduced to maintain the battery at the voltage limit; a reduction in charge current equates to a reduction in the charge accepted by the battery. DCA is thus determined by the difference in the amount of charge accepted by the battery compared to the total available from the charge pulse. All currents used during the microcycle are normalised to the capacity of the battery (C_{exp}), which is obtained experimentally during the test procedure.

Microcycles are applied to the battery in blocks of 20 to form a DCA Pulse Profile (DCAPP). Each microcycle and hence each DCAPP, is inherently energy-balanced. The amount of charge removed during the discharge in step 3 is equal to that accepted by the cell during the charge step, this ensures that the SoC of the battery does not change between the microcycles in the DCAPP.

B. Standard DCA Test A3 Procedure

Figure 3 shows the SoC profile and DCAPP locations as specified by the standard DCA test procedure. The test begins with two heavy discharges to test the reserve capacity performance of the battery, this is followed by a standard-rate discharge to determine C_{exp}. After this preconditioning the battery is recharged to 80% SoC where the first DCAPP

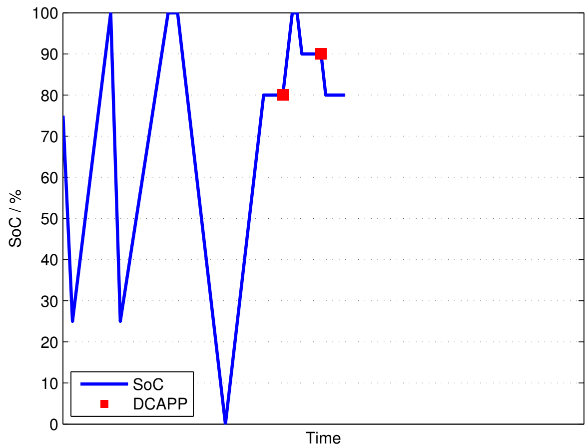

Fig. 3: DCA Test A3 SoC Profile & DCAPP Locations

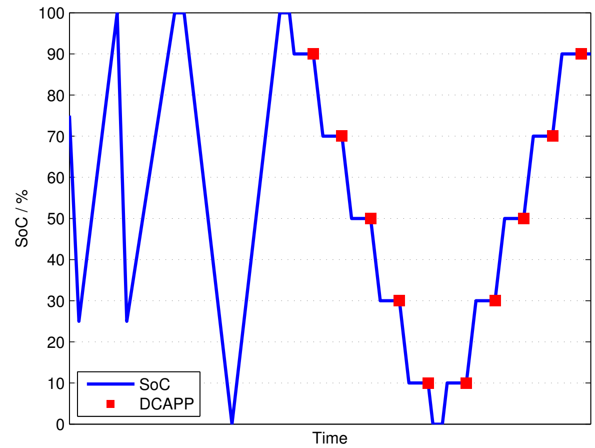

Fig. 4: Modified DCA Test SoC Profile & DCAPP Locations

is performed, this tests the DCA performance of the battery with charge history, i.e. after having been previously subjected to charging. The battery is then fully charged before being discharged to 90% SoC for a second DCAPP, this time testing with discharge history. The test then continues to perform various configurations of simulated drive-cycles, but these are beyond the scope of this work. Throughout the entirety of the test, the battery is maintained at an ambient temperature of 25°C.

C. DCA Calculation

DCA is generally expressed as the average recuperation current (I_{recu}), in units of A·Ah^{-1} [5], for the time of the charge pulse. Thus, for a pulse of arbitrary length, DCA is given by

$$I_{recu} = \frac{Ah_{recu} \cdot 3600}{C_{exp} \cdot t} \tag{1}$$

where Ah_{recu} is the amount charge accepted during the pulse in ampere-hours, C_{exp} is the capacity of the battery in ampere-hours and t is the length of the pulse in seconds.

The DCA Test A3 calculates I_{recu} from the average current of all 20 charge pulses in the DCAPP. As both the length and number of pulses are specified (as 10 s and 20, respectively), this allows for the simplification of (1)

$$I_{recu} = \frac{\left(\sum_{n=1}^{20} Ah_{recu}(n)\right) \cdot 18}{C_{exp}} \tag{2}$$

III. Test Procedure Modifications

The standard DCA Test A3 is somewhat limited in its ability to characterise the DCA performance of batteries as it only performs DCA analyses at two points, both with similar SoC levels. As DCA performance is critical to HEVs and the batteries in HEV applications are likely to be cycled across a wide range of SoC it is important that DCA performance be measured across a similarly wide range. To this end, it is necessary to modify the standard test procedure to better match these requirements.

A. Modified SoC Profile

The modified SoC profile is given in Figure 4. The principal differences are the locations of the DCAPP and the SoC at which they are performed. DCA is measured in 10 places and five SoC across the SoC range, the effects of charge and discharge history are also considered by measuring the DCA at the same SoC with both charge and discharge history. The range of SoC over which the measurements take place are intended to assess DCA performance over a range similar to that of an HEV.

B. Modified DCA Calculation

To better assess the performance of the cells tested, the DCA has been calculated for each charge pulse within the DCAPP, which allows for any trends present during the DCAPP to be identified. To this end the DCA is calculated using an alternative form of (1). Given that the length of the charge pulse is known to be 10 s, the calculation may be adjusted to

$$I_{recu} = \frac{Ah_{recu} \cdot 360}{C_{exp}} \tag{3}$$

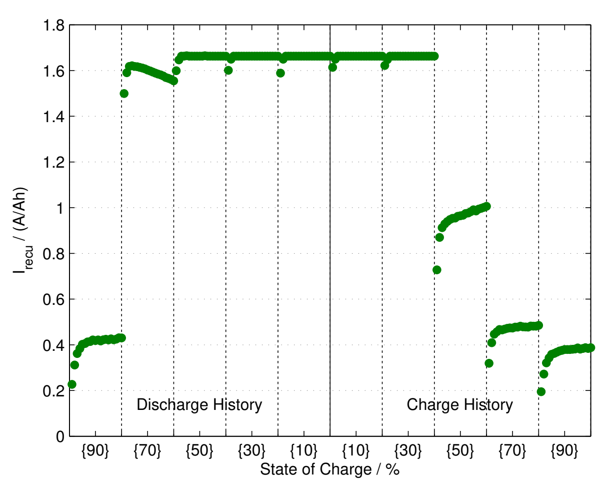

Fig. 5: DCA Performance – Modified SoC Profile, 25°C

Before beginning any discussion of the results, it seems wise to briefly describe the figures used to present said results. The abscissa is divided into 10 discreet sections, one for each SoC of the test procedure. These sections are arranged chronologically from left to right, therefore the centre-line of the axis delineates those results with discharge history on the left from the charge history to the right. Within each section are plotted the DCA results for each microcycle, thus each section contains 20 individual data-points. As with the SoC values, these data-points are plotted chronologically from left to right.

It may be seen from Figure 5 that the modified test profile provides far more information regarding the DCA performance across a range of SoC. Despite this however there is a clear limitation imposed by charge current used, it may be seen that at many of SoC examined the cell is capable of accepting all the charge available and thus the result is artificially limited to the maximum charge current of 1.67 $A{\cdot}Ah^{-1}$.

C. Increased Charge Current

To overcome the limitation discussed above, the microcycle profile is modified to increase the current during the charge (step 1) to 4.00 $A{\cdot}Ah^{-1}$. This value more closely matches the charge currents likely to be experienced by HEV batteries, whilst avoiding excessive stressing of the cells. All other parameters of the microcycle profile remain as indicated in Figure 2 and Table I. Figure 6 shows the results following these modifications.

These results show much more clearly the trend in DCA performance with varying SoC and charge history. The most obvious feature is the variation in DCA with SoC, in broad terms DCA improves with reducing SoC. This is to be expected as the charge capacity of a battery is finite and the further below this limit the present capacity, the more readily charge will be accepted. In this case SoC is analogous to current battery capacity.

By calculating the DCA result for every microcycle, trends within the DCAPP become apparent. In this case there is generally a significant increase in the level of charge acceptance between the first and second pulses, which then reduces as the DCAPP progresses although the general trend of increasing DCA continues. This is more particularly pronounced at lower SoC.

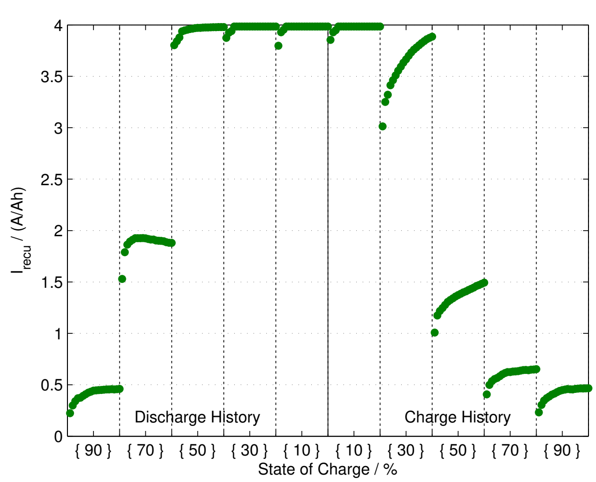

Fig. 6: DCA Performance – Modified Microcycle Profile, 25°C

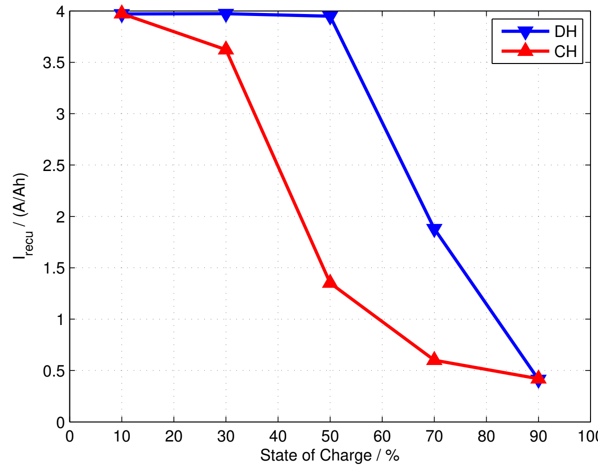

Fig. 7: DCA Variation with Charge History, 25°C

It can also be seen that there are differences in DCA at the same SoC caused by the charge history of the cell. Whilst the results at 90 % SoC correlate well, at all SoC below this, tests with discharge history show significantly improved DCA results. Similar behaviour has previously been observed in lead-acid batteries when subjected to the standard DCA test and similar profiles [5], [7].

To better illustrate this, the results were recalculated using the DCA Test A3 method, as given by (2). This produces a single DCA value for each SoC allowing charge history to be more easily compared. Figure 7 shows the result of this recalculation, clearly showing the effects of charge history. The greatest variation lies within the mid-SoC range, which is the typical range of operation of a HEV battery; thus indicating the need to properly analyse the behaviour of such batteries under these conditions if their real-world performance is to be assessed.

The result also clearly indicates that DCA performance is not merely governed by the SoC of the cell at the time of testing, the electrochemical processes occurring within the cell also affect the results. All testing was carried out following a 1-hour rest period to allow these processes to reach an equilibrium. Despite the rest however, the effect of charge history remains significant, thus it must also be considered as a fundamental factor when assessing DCA performance.

D. Rest Period Variation

Whilst the 30 s rest period specified by the A3 test is fine for determining DCA performance and is necessary for defining a standard test, in real-world applications the rest periods between charge pluses are likely to vary considerably. To assess the effect of this variation on the test cells the microcyle was further modified by altering the length of the rest periods

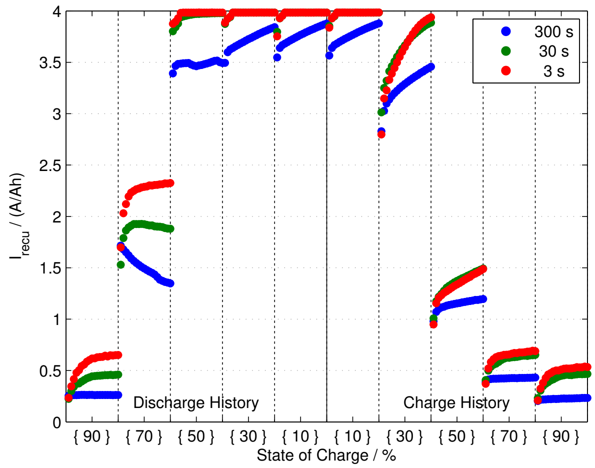

Fig. 8: DCA Variation with Rest Period, 25°C

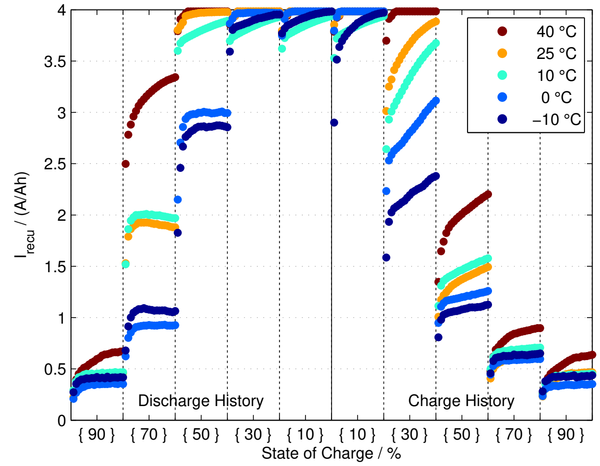

Fig. 9: DCA Variation with Temperature, 30 s Rest Period

used (steps 2 & 4). These were both increased and decreased by one order of magnitude to test cell performance with rest periods of 300 s, 30 s and 3 s; Figure 8 shows the results from this testing.

In this case, the most general observation is that charge acceptance is indeed affected by the rest period. Shorter rests improve DCA performance. It is also apparent that the rest period affects the way charge acceptance changes throughout the DCAPP. With short rest periods the charge acceptance increases more rapidly during the initial pulses before beginning to plateau, as rest period is increased, however, this takes longer to occur. There is also one isolated case (at 70% SoC with discharge history) where the longest rest period lead to a significant decrease in charge acceptance. Investigation of this effect, together with the improvements in performance observed during the initial period of the DCAPP, is ongoing.

Again the effects of charge history are apparent, there is much greater differentiation between rest periods for those results with discharge history. When the cell has charge history however, there is very little difference between the 30 s and 3 s rest periods in either start and end points or shape of the result. This is interesting and suggests that whilst DCA performance is poorer when the cell has charge history, it is also more consistent with regards to rest period.

E. Temperature Variation

As with rest period it is necessary for the A3 Test to fix the ambient temperature during testing to 25°C, in order to define a repeatable standard. However, in practice this will not be the case, instead the batteries in HEVs are subject to significant variations in ambient temperature during their operation. To test performance across a range of temperatures, the test procedure was repeated with the cell at an ambient temperature of -10, 0, 10, 25, or 40°C. These temperatures were chosen to best represent the likely real-world conditions HEV batteries may be exposed to.

Prior to testing the cell was maintained at the test temperature for a period of 24 hours to allow the internal temperature to equalise to that of the ambient. One complete test was then performed before the ambient temperature was adjusted and the cell was again allowed time to equalise. Figure 9 shows the results of this analysis, using the standard rest period of 30 s.

The general trends in the shape of the charge acceptance throughout the DCAPP and the effects of charge history are again present and much as previously identified, the major interest here is the significant effect temperature has on DCA performance. It is well known that the capacity of batteries is reduced as temperature decreases, but the DCA test measures the capacity of the battery at the beginning of the procedure and scales the charge pulses appropriately, so this alone cannot explain the results observed.

The charge storage mechanism within the cell is usually modelled electrically as a pair of series connected capacitors, this equivalent circuit representation is known as the Randles' Model [8] as shown in Figure 10. From the Randles' Model, R_d represents the self discharge resistance of the cell and R_i the resistance of the cell's internal connections, of most interest in this case are C_b, C_s and R_t. C_b is the main charge storage element of the cell, whilst C_s and R_t together model the transient effects of ion concentrations and current densities on the cell plates. C_s is typically several orders of magnitude smaller than C_b [9].

The short-duration, high-current nature of the DCA charge pulse, makes it primarily a test of the surface capacitance of the cell. In fact the DCA profile shares many similarities with a Pseudo-random Binary Sequence (PRBS) profile, which has

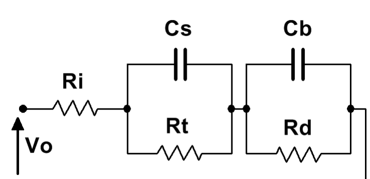

Fig. 10: Randles' Lead-acid Cell Model

been shown to be a good indicator of the values of the discreet components comprising the Randles' model. This testing also showed a significant drop in the value of C_s as temperature is decreased [10]. Clearly a reduction in the surface capacitance will translate into a reduction in the ability of the cell to accept charge.

The reduction in temperature will also affect the value of C_b. This is to be expected as the electrochemical processes with the battery, modelled by C_b, are governed by the Arhennius equation. At lower temperatures the rate of reaction will be slowed, meaning the amount of charge which may be accepted by C_b during the 10 second DCA charge pulse will be reduced [11]. Together these phenomena have the effect of significantly reducing the DCA ability of the cell, as temperature decreases.

IV. Comparison with Standard Lead-Acid

The test methodology described above has been shown to yield informative results regarding the DCA performance of carbon-enhanced lead-acid cells across a range of conditions. This methodology has been extended to investigate the performance of standard lead-acid cells under the same conditions of varied rest period and SoC. The results of the analysis for standard lead-acid are shown in Figure 11. As would be expected they share many similarities with the carbon-enhanced cells, although differences are apparent.

The most obvious difference is in the effect of charge history, this is much more equal for both charge and discharge history, also the trends within each DCAPP exhibit much the same shape (both 30 & 3 s rests being steeper than 300 s) regardless of charge history. It can also be seen that the variation in DCA performance with respect to SoC is more linear for the standard lead than that of the carbon-enhanced. As previously observed DCA is improved with reduced rest periods.

Also apparent is that the reduced effects of charge history come at the expense of DCA performance when the cell has discharge history. It can been seen that for equivalent SoC, with discharge history the DCA performance of standard lead is poorer than that with carbon enhancement.

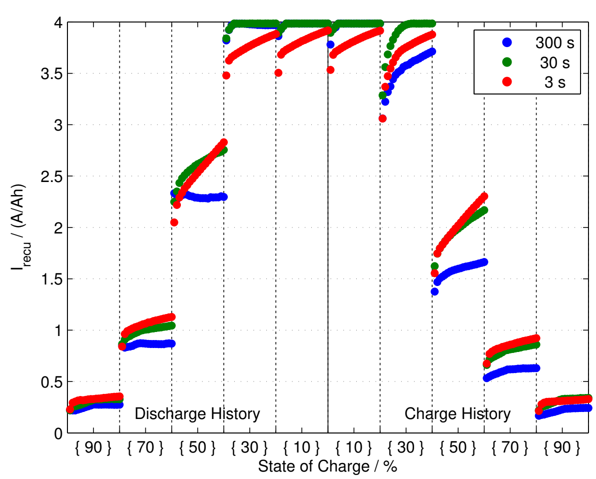

Fig. 11: DCA Analysis Result for Cyclon 2V 2.5Ah standard VRLA cell, 25°C

V. Conclusion

Following the testing of carbon-enhanced lead-acid cells carried out over a range of SoC, rest periods and temperatures there is clear correlation between DCA and both SoC and temperature. DCA is improved at higher temperatures and at lower SoC, furthermore there is some evidence to suggest the cells may exhibit a 'memory effect' leading to improved DCA following a period of discharging. It has also been shown that the rest period used within the test regime significantly affects the DCA response of the cells, in all cases reducing the rest period improves charge acceptance.

These tests also show that DCA is not a static parameter, fundamental to the cell. Rather it is critically dependant on environmental conditions, the history of operations performed on the cell and the electrochemical balance within the cell at any given time. In order to properly understand DCA performance a more thorough test procedure is required than that provided by the A3 Test, one that examines the charge acceptance at various SoC and accounts for the effects of charge history.

Finally the results achieved with carbon-enhanced lead-acid have shown to be largely applicable to standard lead-acid cells, all the trends identified also affect the performance of standard-lead. Carbon-enhancement is seen to improve DCA performance when the cell has discharge history.

References

[1] P. T. Moseley and D. A. Rand, "Partial state-of-charge duty: A challenge but not a show-stopper for lead-acid batteries!" *ECS Transactions*, vol. 41, no. 13, pp. 3–16, 2012.

[2] M. Ehsani, Y. Gao, and J. M. Miller, "Hybrid electric vehicles: architecture and motor drives," *Proceedings of the IEEE*, vol. 95, no. 4, pp. 719–728, 2007.

[3] E. Karden, P. Shinn, P. Bostock, J. Cunningham, E. Schoultz, and D. Kok, "Requirements for future automotive batteries–a snapshot," *Journal of Power Sources*, vol. 144, no. 2, pp. 505–512, 2005.

[4] E. Karden, S. Ploumen, B. Fricke, T. Miller, and K. Snyder, "Energy storage devices for future hybrid electric vehicles," *Journal of Power Sources*, vol. 168, no. 1, pp. 2–11, 2007.

[5] H. Budde-Meiwes, D. Schulte, J. Kowal, D. U. Sauer, R. Hecke, and E. Karden, "Dynamic charge acceptance of lead–acid batteries: Comparison of methods for conditioning and testing," *Journal of Power Sources*, vol. 207, pp. 30–36, 2012.

[6] "DCA Short Test Specification A3, prEN50342-6 – Draft," April 2013.

[7] S. Schaeck, A. Stoermer, J. Albers, D. Weirather-Koestner, and H. Kabza, "Lead-acid batteries in micro-hybrid applications. Part II. Test proposal," *Journal of Power Sources*, vol. 196, no. 3, pp. 1555–1560, 2011.

[8] K. Vetter, *Elektrochemische Kinetik. (German) [Electrochemical Kinetics]*. Springer, Berlin, 1961.

[9] C. R. Gould, C. M. Bingham, D. A. Stone, and P. Bentley, "New battery model and state-of-health determination through subspace parameter estimation and state-observer techniques," *Vehicular Technology, IEEE Transactions on*, vol. 58, no. 8, pp. 3905–3916, 2009.

[10] A. Fairweather, M. Foster, and D. Stone, "Modelling of VRLA batteries over operational temperature range using pseudo random binary sequences," *Journal of Power Sources*, vol. 207, pp. 56–59, 2012.

[11] T. Sharpe and R. Conell, "Low-temperature charging behaviour of lead-acid cells," *Journal of Applied Electrochemistry*, vol. 17, no. 4, pp. 789–799, 1987.